Ultraviolet absorption observations of intermediate-velocity cloud gas detected towards the M 15 globular cluster

Barry Y. Welsh, Jonathan Wheatley, Rosine Lallement

A&A 537, A51 (2012)
DOI: 10.1051/0004-6361/201118063

Astronomy & Astrophysics

Ultraviolet absorption observations of intermediate-velocity cloud gas detected towards the M 15 globular cluster

B. Y. Welsh[1], J. Wheatley[1], and R. Lallement[2]

[1] Space Sciences Laboratory, University of California, 7 Gauss Way, Berkeley, CA 94720, USA
e-mail: bwelsh@ssl.berkeley.edu
[2] IPSL/LATMOS, Versailles, France

Received 9 September 2011 / Accepted 4 November 2011

ABSTRACT

Aims. We present medium resolution ultraviolet interstellar absorption measurements recorded with the HST-COS and FUSE spectrographs towards two post-AGB stars (K 559 & K 648) located within the M 15 globular cluster ($l \sim 65°$, $b \sim -27°$). By sampling interstellar gas over the 10.4 kpc sight-line towards M 15 we wish to reveal spectral features that are associated with absorption due to the foreground g1 intermediate velocity cloud (IVC), whose distance has previously been constrained to lie between 1.8–3.8 kpc.
Methods. Inspection of the UV line profiles recorded towards both stars have revealed measurable IVC absorption at $V_{\rm lsr} \sim +61.5 \pm 5$ km s^{-1} in the profiles of the CI, CII, CII*, CIV, NI, NII, OI, OVI, AlII, SiII, SiIII, SiIV, PII, SII, FeII, FeIII and NiII ions. Line-profile fitting to the IVC absorption features has resulted in column density determinations for the low and high ions. The best-fit column density values for the various ions have near identical values along *both* sight-lines, such that our UV data does not reveal the significant small-scale structure that has been reported previously for the g1 cloud.
Results. The observed column density ratios of the CIV, SiIV, OVI and NV IV components are consistent with what may be expected from turbulent mixing layers, shock ionization or halo SNR models, although no one model can predict all of the observed ratios. We derive sub-solar metallicity values of [O/H] = -1.22 ± 0.44 and [N/H] = -1.21 ± 0.38 for the neutral IVC gas, and also the IV components of C, Si, Al, Ni and Fe mainly possess less than solar abundance ratios relative to that of N. A possible origin for the g1 IVC is that of a low metallicity cloud that has been accreted towards our galaxy, has passed through the disk and is now moving away from the galactic plane.

Key words. ISM: clouds – ISM: abundances – galaxies: halos

1. Introduction

Over the past decade much progress has been made in furthering our understanding of the distribution and physical/chemical properties of interstellar gas located in the galactic halo through ultraviolet absorption studies using spectrographs flown aboard the NASA Far Ultraviolet Spectroscopic Explorer (FUSE) and *Hubble* Space Telescope (HST) satellites (Richter et al. 2001b; Sembach et al. 2003; Savage et al. 2003; Savage & Wakker 2009; Lehner & Howk 2010). These, and many other, studies have shown that the gas surrounding our Galaxy has a wide range of temperature and ionization states consisting of cold and neutral, warm and neutral, warm and ionized, and hot and ionized interstellar gas. These various phases of the halo gas each have different scale-heights above the plane, with the highly ionized phase being the most extended and reaching to a z-height of ~4 kpc (Savage & Wakker 2009). Immersed within the halo are the intermediate velocity clouds (IVCs), which are (historically) defined by their neutral hydrogen radial velocities of $|V_{\rm LSR}| = 30$–90 km s^{-1} (Wakker 1991). Although originally thought to be mainly neutral gas entities (as traced by HI and molecular H_2), these gas clouds have also been shown to contain ionized and highly ionized species and, as such, can be considered as "multi-phase" interstellar features (Danly et al. 1992; Richter et al. 2001a; Shull et al. 2009). The IVCs are a key component of the interstellar gas since they contain a significant percentage of the kinetic energy of the neutral medium and are thought to play an important role in the galactic star formation process. In most galactic evolution models the infall of a reservoir of low-metallicity gas is required to provide fuel for subsequent generations of star formation and to account for the observed metallicity value of G and K stellar dwarfs (Flynn & Morell 1997). In the galactic fountain model hot and highly ionized gas is ejected away from the galactic disk by supernovae explosions, with such gas eventually falling back into the plane in the form of cooled and condensed neutral gas clouds moving with intermediate (and high) velocities (Shapiro & Field 1976; Bregman 1980). Since galactic fountain gas is thought to be metal rich, we might therefore expect IVC gas also to exhibit a metallicity value near to that of solar, which has indeed been found for several (but not all) IVCs (Wakker 2001; Richter et al. 2001b). Additionally, we would also expect IVCs to be located within the lower galactic halo ($z \lesssim 3$ kpc), over distances where the energetics of the galactic fountain infall process are thought to operate (Spitoni et al. 2008). Although distances to several IVCs currently exist (Wakker 2001; Wakker et al. 2008), such values are sometimes poorly constrained, often due to the paucity of suitable background targets towards which interstellar absorption measurements can be made.

With the recent launch of the Cosmic Origins Spectrograph (COS) (Osterman et al. 2011) aboard the HST, this new ultraviolet (UV) spectrograph allows us to probe (faint) UV-bright post-AGB stars belonging to globular clusters in the 5–15 kpc distance range, such that the chemical composition of foreground IVCs (and high velocity clouds, HVCs) can be revealed through study of their interstellar absorption line profiles.

High-velocity and/or intermediate-velocity gas has recently been detected along 3 different stellar sight-lines using this instrument, with the various absorptions arising in interstellar clouds lying within 1–15 kpc distance range (Lehner & Howk 2010; Yao et al. 2011; Welsh et al. 2011). Our present paper deals mainly with HST-COS observations of the sight-lines towards two (ultraviolet-bright) post-AGB stars (K 559 and K 648) belonging the M 15 ($l = 65°$, $b = -27.3°$) globular cluster that pass through a previously known foreground IVC feature named the g1 cloud. An IVC was first detected towards M 15 at $V_{\rm lsr} \sim +65$ km s^{-1} by Kerr & Knapp (1972) using HI 21cm emission observations, and since then various optical absorption studies of stellar targets along the M 15 sight-line have provided a distance estimate to the g1 cloud of 1.8 to 3.8 kpc (Lehner et al. 1999; Wakker et al. 2008). The interstellar sight-lines towards K 559 and K 648 have also been studied at high spectral resolution in both the NaI and CaII visible absorption lines by Welsh et al. (2009) and Smoker et al. (2002a). These optical observations have revealed the IVC to consist of at least two absorption components with average gas velocities of $V_{\rm lsr} = +66$ km s^{-1} and $V_{\rm lsr} = +55$ km s^{-1}, as seen in the interstellar CaII K-line profiles. The absorbing gas within this 3 deg^2 IVC has also been shown to exhibit significant small-scale structure, with the NaI interstellar column densities varying by up to a factor of 16 over scales of 3 arcmin in the foreground cloud (Meyer & Lauroesch 1999).

Our new UV observations are presently aimed at determining the gas phase abundances of the various ion species recorded in absorption at the velocity of the sight-line IVC. From these data we derive metallicity values for the IV gas in the g1 cloud, which attempt to constrain its possible origin with regards to gas expelled from (and returning to) the galactic disk.

2. Observations and analysis

As part of the NASA HST Cycle 17 COS guaranteed time observation program GTO-11527, we observed the UV-bright post-AGB star K 559 (also known as M 15-Zng1) on 24 October 2010 and the CSPN star K 648 (Bianchi et al. 2001) on 13 November 2010. Both stars are members of the M 15 (NGC 7078) globular cluster with a nominal distance of 10.4 ± 0.8 kpc (Durrel & Harris 1993). The relevant astronomical information for both stellar targets are presented in Table 1, with the data for K 559 being taken from Mooney et al. (2004) and the data for K 648 from Bianchi et al. (2001). The photon data were taken through the 1 arcsec COS prime science aperture, with the UV light being dispersed with the G130M and G160M diffraction gratings during respective exposure times of 1712 s and 2545 s for K 559 and 1628 s and 2545 s for K 648. The dispersed photons were recorded with a micro-channel plate detector operated in the time-tag mode (see Osterman et al. 2011, for a detailed description of the HST-COS instrument). The data were extracted using the latest version of the CALCOS pipeline software, resulting in spectra covering the wavelength range 1170–1750 Å recorded at a resolving power of $R \sim 20\,000$ (~15 km s^{-1}). The accuracy of the wavelength scale of the UV spectra is ±3 km s^{-1}, which degrades by ~factor two at the extremes of the spectral range, and all data in this paper are presented in the LSR velocity scale. Typically, the resultant S/N ratio for most of these spectral data is >15:1.

In order to broaden the utility of the COS data, we have also used the FUSE spectrum of K 648 (data set D1570101000), which has been downloaded from the Multi-Mission Archive at the Space Telescope Institute. There is no equivalent FUSE spectrum for the star K 559. The far UV spectrum of K 648 has a S/N ratio >10:1 for wavelengths >1000 Å, but has a complex continuum composed of many stellar and molecular absorption lines. However, this spectrum has proven useful as a check on the reality of absorption features seen in the profiles of ions that possess transitions in both of the HST-COS and FUSE band-passes (e.g. OI, NI and FeII), in addition to allowing the analysis of a few absorption lines observed only at wavelengths <1150 Å (i.e. OVI λ1032 Å and NII λ1084 Å).

Obtaining a priori knowledge of the theoretical spectrum expected from a post-AGB star is highly desirable for our spectral analysis, since the underlying stellar UV spectra of K 559 and K 649 both contain many relatively narrow absorption features that can easily be misidentified as interstellar absorption lines. Thus, we have made use of the stellar atmosphere models of Dixon et al. (2011) as an aid in the interstellar identification process. For an example of post-AGB stellar lines masquerading as interstellar features see Fig. 1 of Welsh et al. (2011). Fortunately the radial velocity of M 15 (and its stellar members) is $V_{\rm lsr} \sim -100$ km s^{-1} (Drukier et al. 1998), which for most unsaturated interstellar absorption lines is well removed from the absorption due to the galactic disk (at $V_{\rm lsr} \sim 0$ km s^{-1}) and also any absorption expected from the g1 IVC with velocities near $V_{\rm lsr} \sim +65$ km s^{-1}.

We derive normalized intensity profiles for the interstellar UV lines of interest by fitting the local stellar continua with a multi-order polynomial fit typically over a range of ±250 km s^{-1} from the center of the line absorption. The main absorption component for all ions is centered at ~0 km s^{-1} (see Figs. 1 and 2), and is due to line-of-sight absorption from the ISM in the galactic disk and will not be discussed further. Absorption from IV gas with an average velocity of $V_{\rm lsr} = +61.5 \pm 6$ km s^{-1} was detected and deemed to be measurable in the UV line profiles of the CI, CII*, CIV, NI, NII, OI, OVI, AlII, SiII, SiIV, PII, SII, FeII and NiII ions seen towards K 648 (see Table 2). Similarly, for the K 559 sight-line an IVC at an average velocity of $V_{\rm lsr} = +61.5 \pm 5$ km s^{-1} was detected in the CI, CII, CII*, CIV, NI, OI, AlII, SiII, SiIII, SiIV, PII, SII, FeII, FeIII and NiII ions. We note that these (near identical) IVC velocity values are close to the average velocity value of the two absorption components measured (at higher spectral resolution) in the CaII K-line by Welsh et al. (2009) and Smoker et al. (2002a). This IVC component is also revealed at a velocity of $V_{\rm lsr} = +69$ km s^{-1} in the HI 21cm emission profile recorded towards the central region of M 15 by Kennedy et al. (1998).

2.1. Absorption profile fitting

When present in the UV spectra, we have fit each of the IV components with a theoretical Voigt absorption model, defined by an ion column density (N), a doppler b-value and a cloud velocity ($V_{\rm lsr}$), using a least-squares minimization line profile fitting routine fully described in Vallerga et al. (1993) and Welsh & Lallement (2005). Since an undetermined value of non-thermal broadening (i.e. turbulence) dominates the observed line-widths of IVC (and HVC) profiles in the ultraviolet (Howk et al. 2003), the allowable model doppler line-width values (broadened by the instrumental resolution of HST or FUSE) require some constraint. For the IV components detected in the (generally unsaturated) lower ionization ions of SII, FeII and SiII we presently restrict the best-fit doppler widths to values of $11 < b < 14.0$ km s^{-1} (i.e. $b = 12.5 \pm 1.5$ km s^{-1}). This range of values is very similar to that determined for fitting other IVC and HVC components observed with a similar spectral resolution in

Table 1. Stellar target information.

Name	RA (2000.)	Dec (2000.)	m_v	Sp	Temp (K)	$V_{*\mathrm{LSR}}$ (km s^{-1})	COS data sets
K 559	21:29:58.19	+12:11:42.5	14.8	post-AGB	28 000	–100	LB2403010/020
K 648	21:29:59.40	+12:10:26.0	14.7	post-AGB/CSPN	37 000	–140	LB2402010/020

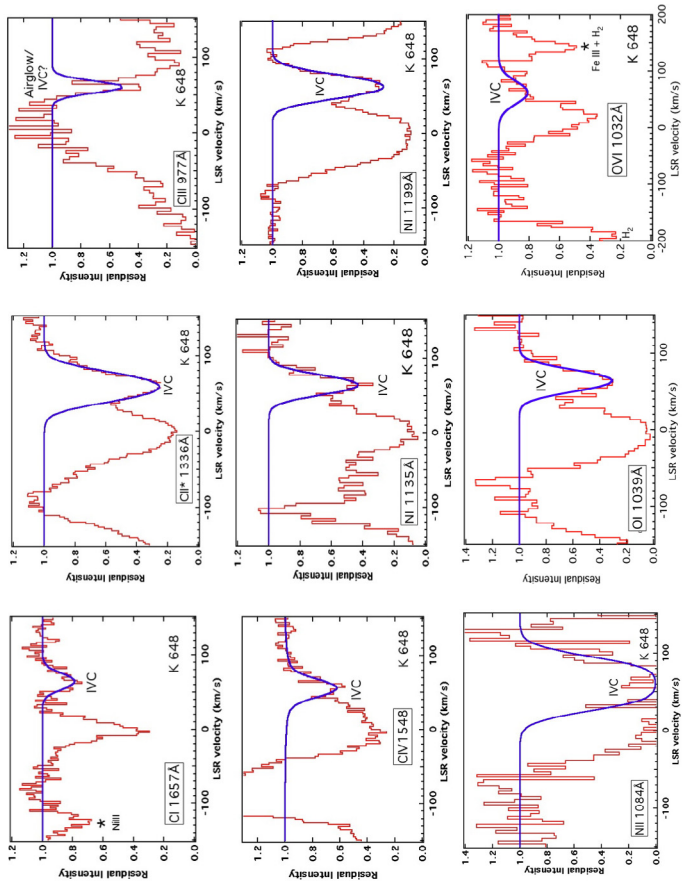

Fig. 1. Normalized UV absorption line profiles of the CI, CII*, CIII, CIV, NI, NII,OI and OVI ions exhibiting measurable IVC absorption towards the star K 648 at a velocity of $V_{\mathrm{lsr}} \sim +61.5$ km s^{-1}. The position of the IVC gas is shown for each profile (IVC) and any stellar features are marked with an asterisk. The best-fit model to the IV absorption components are shown by the thick lines.

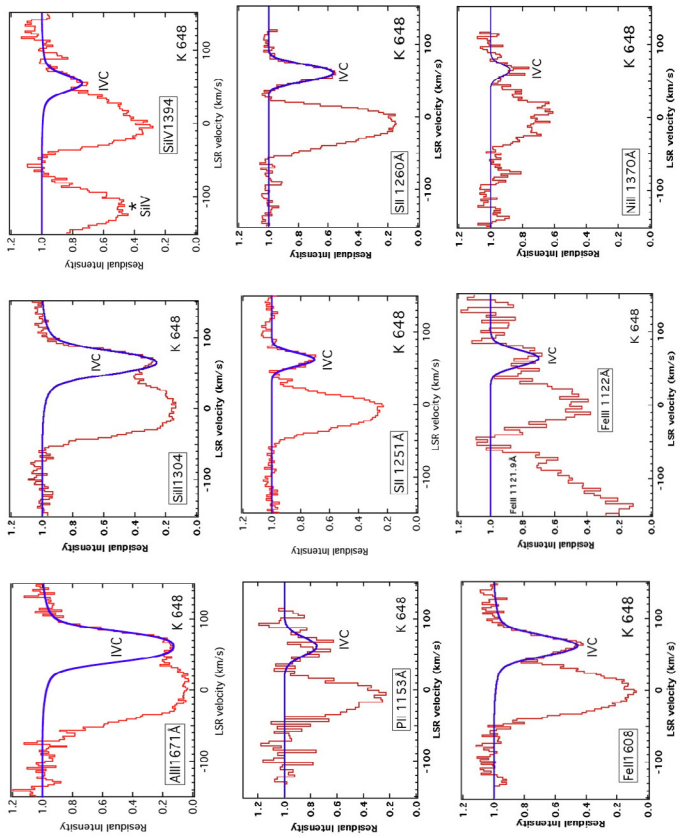

Fig. 2. Normalized UV absorption line profiles of the AlII, SiII, SiIV, PII, SII, FeII, FeIII and NiII ions exhibiting IVC absorption towards the star K 648 at a velocity of $V_{\mathrm{lsr}} \sim +61.5$ km s^{-1}. See Fig. 1 for further details.

the ultraviolet (Collins et al. 2004; Yao et al. 2011; Welsh et al. 2011). No similar constraint was placed on the allowable doppler widths for the higher ionization ultraviolet lines. The best-fit values of V_{lsr}, b and N for the IVC components detected towards both stars are listed in Table 1. The corresponding absorption model fits are shown in Fig. 1 (for K 648) and Fig. 2 (for K 559) superposed on the observed residual intensity profiles.

The errors for the column density values listed in Table 2 represent one-sigma deviations from the constrained best-fit doppler-widths. For the case of NII λ1084 Å the IV component fit has been numerically constrained by the shape of one of its absorption wings and thus the error on the model fit is larger than that derived for IV components that are well isolated from the main absorption at $V_{\mathrm{lsr}} = 0$ km s^{-1}. We note that the CIII λ977 Å line in the FUSE spectrum of K 648 is contaminated by geocoronal emission. Although an IVC absorption feature at $V_{\mathrm{lsr}} \sim +61$ km s^{-1} is seen within the line profile, we prefer to consider this as a conservative upper limit to the value of N(CIII) along this sight-line. For completeness we also list the column density values for the interstellar NaI λ5890 Å and CaII λ3393 Å lines observed towards both K 648 and K 559 by Welsh et al. (2009). We also list the HI column density value for K 648 as determined by Kennedy et al. (1998) for the center of M 15 ($l = +65.0°$, $b = -27.3°$) using the Lovell radio telescope (12 × 12 arcmin beam), and for K 559 (Zng-1) as determined by Smoker et al. (2002a) using a combined Arecibo-Westerbork Synthesis map of spatial resolution 2 × 1 arcmin.

In Table 2 we list our derived best-fit model values of V_{lsr}, b and N for each ion in which an IVC component was detected with confidence towards K 559 and K 648. The error listed for the column densities represent one-sigma deviations from the constrained best-fit doppler-widths. In several cases the IV component is blended with the main (line-of-sight) absorption component at $V \sim 0$ km s^{-1}), such that the line-fit model is constrained only by the shape of one its absorption wings. Thus, the errors associated with the model column density fit for these

Table 2. Intermediate velocity absorption component best-fits for K 648 and K 559.

Spectral line	K 648 Line velocity (km s^{-1})	K 648 *b*-value (km s^{-1})	K 648 Log Col density (N)	K 559 Line velocity (km s^{-1})	K 559 *b*-value (km s^{-1})	K 559 Log Col density (N)
HI (radio 21 cm)	+69.0		19.60 ± 0.3	+69.0		19.70 ± 0.3
NaI 5890 Å:.	+60.5	6.5	11.45 ± 0.07	+67.0	2.6	11.83 ± 0.04
CaII 3393 Å:.	+58.5	6.4	11.82 ± 0.05			
	+68.4	3.1	12.33 ± 0.04	+65.0	5.5	12.30 ± 0.04
CI 1157 Å:..	+64.1	13.0	13.01 ± 0.03	+64.5	12.5	13.08 ± 0.05
CII 1335 Å:..	***	***	***	+59.0	20.0	15.06 ± 0.15
CII* 1336 Å:..	+58.5	14.0	14.10 ± 0.10	+61.0	12.5	14.07 ± 0.10
CIII 977 Å:..	+60.5		<13.09	N/A	N/A	N/A
CIV 1548 Å:..	+58.5	14.5	13.35 ± 0.05	+58.0	15.0	13.33 ± 0.06
CIV 1551 Å:..	+58.0	14.5	13.35 ± 0.06	+61.0	15.0	13.39 ± 0.08
NI 1135 Å:..	+63.5	13.5	14.29 ± 0.10	N/A	N/A	N/A
NI 1199 Å:.	+61.5	14.0	14.25 ± 0.08	+62.0	15.0	14.23 ± 0.07
NI 1201 Å:.	+65.5	14.0	14.24 ± 0.08	+61.0	14.5	14.33 ± 0.06
NII 1084 Å:..	+60.5	20.0	14.86 ± 0.2	N/A	N/A	N/A
NIII 989 Å:.	***	***	***	N/A	N/A	N/A
NV 1239 Å:..			<12.34			<12.70
OI 1039 Å:..	+64.0	13.5	15.16 ± 0.12	N/A	N/A	N/A
OI 1302 Å:..	+64.0	14.5	15.06 ± 0.15	+63.0	14.5	15.14 ± 0.15
OVI 1032 Å:..	+62.0	25.0	13.44 ± 0.10	N/A	N/A	N/A
AlII 1671 Å:..	+62.0	13.5	13.38 ± 0.10	+60.0	15.0	13.29 ± 0.08
SiII 1304 Å:..	+64.0	14.0	14.25 ± 0.06	+60.5	14.0	14.25 ± 0.06
SiII 1527 Å:..	+62.0	14.0	14.26 ± 0.08	+64.5	14.0	14.27 ± 0.06
SiIII 1206 Å:..	***	***	***	+62.5	18.0	13.26 ± 0.10
SiIV 1394 Å:..	+55.0	15.5	12.72 ± 0.05	+55.0	17.0	12.83 ± 0.10
SiIV 1403 Å:..	+55.0	15.5	12.81 ± 0.06	+55.0	15.0	12.70 ± 0.12
PII 1153 Å:..	+63.0	14.0	13.07 ± 0.06	+64.5	12.5	13.11 ± 0.06
SII 1251 Å:..	+62.5	12.0	14.54 ± 0.06	+65.0	12.5	14.58 ± 0.05
SII 1254 Å:..	+62.5	12.0	14.51 ± 0.06	+62.5	13.0	14.61 ± 0.05
SII 1259 Å:..	+64.0	13.0	14.58 ± 0.06	+62.0	13.0	14.64 ± 0.05
FeII 1143 Å:.	+63.0	13.5	14.18 ± 0.07	+60.0	12.0	14.11 ± 0.06
FeII 1145 Å:..	+60.0	12.5	14.26 ± 0.08	+61.0	12.5	14.23 ± 0.08
FeII 1608 Å:..	+62.5	13.5	14.11 ± 0.06	+61.5	12.5	14.19 ± 0.06
FeIII 1122 Å:.	+62.0	12.5	13.77 ± 0.06	N/A	N/A	N/A
NiII 1370 Å:.	+65.0	11.0	12.92 ± 0.07	+63.0	11.0	12.99 ± 0.10

Notes. N/A = no FUSE spectral data available for this absorption line. *** = IV absorption present, but profile too blended or saturated to obtain a well-constrained fit. all velocities are in the LSR scale.

profiles are larger than for lines in which the IV component is well removed from the main central absorption. The fact that our derived fit for the well removed IVC component seen in the OI λ1039 Å line towards K 648 gives very similar model fit results to that of the blended IVC component seen in the OI λ1302 Å line gives us confidence that our profile fit method is robust, even in cases of modest component blending. Due to strong saturation and line blending effects we have been unable to fit the CII λ1335 Å and SiIII λ1206 Å IVC component recorded towards K 648, although absorption at the IVC velocity is present in both line profiles.

2.2. Profile fit overview and adopted column density values

The results presented in Table 2 show that the IVC component is detected at a near identical average velocity of $V_{\rm lsr} \sim +61.5$ km s^{-1} towards both of the M 15 stellar members. However, we note that there is difference of ∼–7.5 km s^{-1} between the average IVC velocity of $V_{\rm lsr} = +61.5$ km s^{-1} derived from the present UV data, and that of $V_{\rm lsr} = +69$ km s^{-1} gained from radio HI observations (whose velocity resolution is typically ∼1 km s^{-1}). We can attribute this velocity difference to the fact that the high spectral resolution visible CaII K-line

Table 3. Adopted average* component best-fits for the g1 IVC.

Ion species	Av. line velocity (km s^{-1})	Av. log Col density
HI (radio 21 cm)	+69.0	19.65 ± 0.3
CI	+64.3	13.35 ± 0.04
CII	+59.0	15.06 ± 0.15
CII*	+60.0	14.09 ± 0.10
CIII ...	+60.5	<13.09
CIV...	+59.0	13.36 ± 0.06
NI	+62.5	14.27 ± 0.08
NII	+60.5	14.86 ± 0.2
NIII ...	N/A	N/A
NV....		<12.34
OI....	+63.5	15.12 ± 0.14
OVI....	+62.0	13.44 ± 0.10
AlII....	+61.0	13.34 ± 0.09
SiII....	+63.0	14.26 ± 0.06
SiIII....	+62.5	13.26 ± 0.10
SiIV....	+55.0	12.77 ± 0.08
PII....	+63.5	13.09 ± 0.06
SII	+63.0	14.58 ± 0.06
FeII ...	+61.0	14.18 ± 0.07
FeIII...	+62.0	13.77 ± 0.06
NiII....	+64.0	12.96 ± 0.08

Notes. * = Values averaged over the two M 15 sight-lines. All velocities are in the LSR scale.

observations towards both stars by Welsh et al. (2009) revealed a two-component IVC absorption structure (at $V_{\rm lsr}$ = +55 and +65 km s^{-1}), which the lower resolution HST-COS observations are unable resolve and thus the IVC line-center is biased towards the lower velocity in the present data.

Table 2 also shows that the best-fit column density values for the various ions have near identical values (within the quoted errors) along both of the sampled sight-lines. The similarity of these fit data provides us with confidence in the fitting method we have used for some of the more complex profiles in which only a limited portion of the IVC absorption profile was available for modeling. Since, within the errors, the derived IVC column density values are so similar for the ions observed towards both stars, in Table 3 we list the adopted "average" UV ion column density values (and cloud velocities) that will be used throughout the following discussion, particularly in Sect. 3.3. For cases where an ion column density is measured towards one star but not the other, we adopt the measured value of column density (N) as being valid within the quoted error for both stellar sight-lines.

3. Discussion

Many observations have focussed on the UV absorption characteristics of gas originating within HVCs (Sembach et al. 1999; Gibson et al. 2001; Collins et al. 2003; Yao et al. 2011; Shull et al. 2011; and Welsh et al. 2011). These, and many other studies, have generally shown the HVCs to be multiphase interstellar structures with distances >5 kpc and containing interstellar gas with (sub-solar) metallicities ranging from 10–30% solar. Our present UV data reveals that the g1 IVC is also a multiphase entity that contains neutral gas (as traced by NaI, HI , CI, NI and OI), in addition to the presence of highly ionized gas regions (as traced by SiIV, CIV and OVI). We note that Shull et al. (2009) has found that >80% of the high latitude sky contains ionized SiIII λ1206.5 gas regions, the majority of which are infalling clouds. This "layer" of ionized, low-metallicity gas in the lower galactic halo is thought to be a reservoir of cooling inflowing gas that could potentially replenish the star formation process in the disk. However, the predicted velocity of the g1 cloud (due to galactic rotation) is $V_{\rm lsr}$ ~ +19 km s^{-1} with respect to the Sun (Little et al. 1994), which implies that the IVC gas detected towards M 15 is *outflowing* into the halo rather than inflowing towards the disk. Although other IVCs, such as those seen towards M 55 (Lyons et al. 1994) and towards the Magellanic Bridge (Lehner et al. 2001), have also been shown to possess clouds of outflowing gas, the present high sensitivity UV data in the sight-line to M 15 affords us with the opportunity to sample the chemical and physical characteristics of the less-studied outflowing gas associated with IVCs in the lower halo.

3.1. IVC small-scale structure

The extent of the g1 IVC on the sky, as mapped by HI, is ~2.5° × 2.0° (Kennedy et al. 1998). The two targets stars, K 559 and K 648, have sight-lines that are only ~1.3 arcmin apart and, although significant small-scale structure in the NaI lines has been observed at a spatial resolution of 4 arcsec towards the very central 27 × 43 arcsec region of the M 15 cluster by Meyer & Lauroesch (1999), our UV observations (sampled within a 1 arcsec field of view along sight-lines that are ≳30 arcsec away from the cluster center) do not reveal these large column density variations in the presently sampled IVC gas. Parenthetically, we note that our own high resolution NaI observations of these two stars also revealed a variation of a factor 2.3 in the observed column density values (Welsh et al. 2009). The 21 cm HI observations of the M 15 region by Smoker et al. (2002b) have similarly shown variations in the HI column density value by a factor of ~4 on scales of ~5 arcmin, which corresponds to spatial scales of <5 pc in the foreground IVC gas. The difference between the findings derived from the NaI/HI radio and our UV data could be that the UV lines sample a far wider range of temperature, ionization and velocity than the NaI and HI (neutral gas) observations (i.e. significant amounts of unobserved NaII and HII may exist), or that regions further away from the cluster center do not exhibit particularly high levels of small-scale density structure.

3.2. The highly ionized IVC gas

Highly ionized IVC gas has been detected along the sight-lines towards both stars in the line profiles of both the CIV and SiIV ions, and towards K 648 in the absorption profile of OVI. Previous studies of HVC gas suggest that photoionization (by radiation from the extragalactic background and the radiation field escaping from the Milky Way) can generally account for the observed absorption levels of the lower ionization lines (e.g. SiII, FeII, CII, etc.), but it cannot account for the observed levels of the high ions of CIV, SiIV and OVI (Fox et al. 2005; Collins et al. 2007; Shull et al. 2011; Welsh et al. 2011). The highly ionized IVC component can best studied through comparison of the high-ion column density ratios of CIV, SiIV, NV (upper limits) and OVI, which act as a diagnostic of the ionization processes that may be operating in the IVC gas. These processes may include radiative cooling, conductive interfaces, turbulent mixing layers, shock ionization and ionization by halo SNR bubbles and have been discussed for several interstellar environments by Indebetouw & Shull (2004). However, observations of the gas in HVCs indicate that the ionized component in these fast-moving clouds is not in equilibrium (Sembach et al. 2002; Fox et al. 2005), and non-equilibrium processes such as time-dependent

radiative cooling, shock ionization or ionization in conductive interfaces are favored to operate instead within these environments. For the case of the M 15 sight-line absorption by high ions at the velocity of the IVC suggests the presence of a highly ionized boundary to the g1 cloud due to its interaction with the surrounding halo gas as it flows outward and away from the disk. Hence, we would expect that some form of collisional ionization model (such as turbulent mixing layers or shock ionization) would be appropriate to explain our observed high ion data.

The predicted high ion column density ratios for five potential ionization processes are listed in Table 7 of Zech et al. (2008), and are reproduced in our Table 4 for comparison purposes with the present g1 cloud values. Using the column densities listed in Table 3 we derive measured ratio values of N(CIV)/N(SiIV) = 3.9 ± 1.5, N(CIV)/N(OVI) = 0.83 ± 0.37 and N(CIV)/N(NV) > 10.5 for the IV gas towards M 15. Also included in Table 4 are values for these ratios as recorded in HVCs towards M 5 (Zech et al. 2008) and in the Complex M HVC detected towards Mrk 421 (Yao et al. 2011). We note that there are no published column density data for simultaneous detections of intermediate-velocity SiIV, CIV, NV and OVI along any IVC sight-line (Wakker, B., priv. comm.). This is mainly due to the intrinsic width of the high ion absorption component being similar to, or larger than, the separation in velocity between the (strong) local ($V \sim 0$ km s^{-1}) and IV absorption components.

Although our present high ion ratios (for an IVC) appear to fit some of the predicted HVC column density ratios listed for various models in Table 4, we note that care must be taken in recognizing the input parameters (such as solar abundance ratios, metallicity and age of the gas cloud) that were used in each particular ionization model. The various model constraints for each of the 5 ionization models are listed in Table 7 of Zech et al. (2008). We also note that Fox et al. (2005) claim to match the observed high ion ratios in 11 out of 12 cases of ionized HVCs using a magnetized conductive interface model of Borkowski et al. (1990). But recent non-equilibrium model calculations by Gnat, Sternberg & McKee (2010) for thermally conductive interfaces surrounded by warm, photo-ionized (halo) gas are unable to reproduce the OVI column densities that are widely found in HVCs. Clearly, more work is required to resolve this apparent disconnect with regards to interface models, although the underprediction of OVI can be alleviated if multiple interfaces exist along the sight-line. Kwak & Shelton (2010) and Kwak et al. (2011) have recently run hydrodynamic simulations of HVCs traveling through a hot tenuous medium in the galactic halo to predict the expected HI and high ion column densities as a function of evolutionary time. Although these turbulent mixing models are best suited for clouds with velocities >100 km s^{-1}, similar ratios are predicted for the slightly lower g1 cloud velocity (Shelton, private communication). The model N(CIV)/N(OVI) ratios (as shown in Fig. 12 of Kwak et al. 2011) are consistent with the presently observed ratio value of 0.83 ± 0.37, but (like the conductive interface models) the actual predicted column density of OVI is under-predicted. Also, our observations reveal (slightly) more SiIV to CIV and more CIV to NV than the time-averaged models currently predict (Shelton, priv. comm.).

Although it is beyond the scope of this paper to critique the many input assumptions of the various interstellar ionization models, the reader should apply "caveat emptor" in deciding which model best fits the observations. With this in mind, the three column density ratio values we have determined for the g1 IV cloud are mainly consistent with what may be expected from turbulent mixing layers, shock ionization and halo SNR, although no one model is able to predict *all* of the high ion column

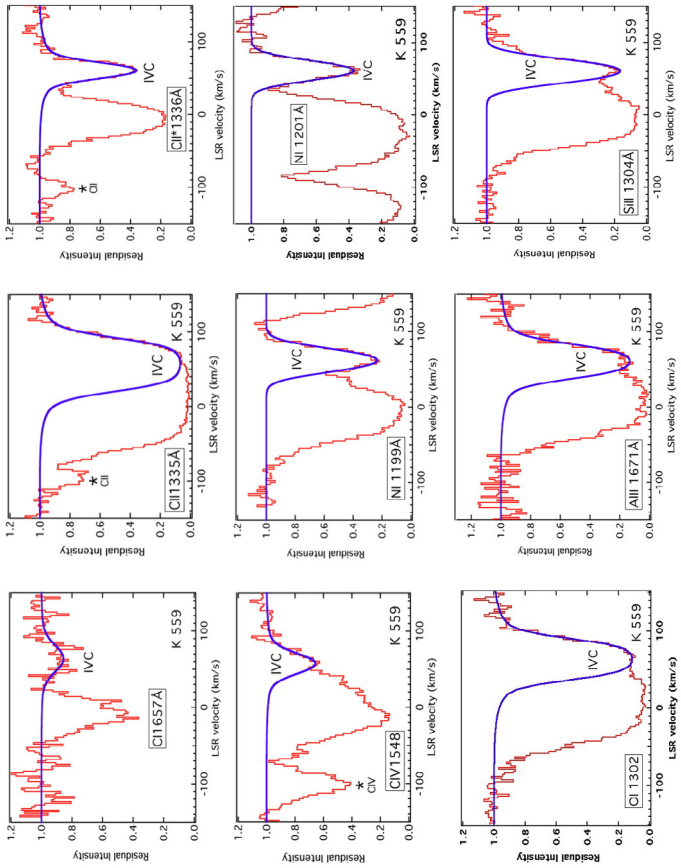

Fig. 3. Normalized UV absorption line profiles of the CI, CII, CIV, NI, OI, AlII and SiII ions exhibiting IVC absorption towards the star K 559 at a velocity of $V_{\rm lsr} \sim +61.5$ km s^{-1}. See Fig. 1 for further details.

density ratios. A similar result was also been found for the HVC gas detected towards M 13 (Welsh et al. 2011) and M 5 (Zech et al. 2008). Thus, at least in this particular sight-line, the high ion ratios seen in HVCs are comparable to those seen in an IVC.

3.3. IVC gas-phase abundances and possible origin

As discussed in the Introduction, knowledge of the metallicity and distance of an IVC can provide important constraints on the possible origin and history of its constituent gas. The OI and HI ions have near identical ionization potentials and the column density ratio of N(OI)/N(HI) has been widely used as a metallicity estimator, defined as [O/H], for the *neutral* gas found in both IVCs and HVCs (Collins et al. 2003; Zech et al. 2008; Tripp & Song 2007). Although there is certainly substantial amounts of ionized gas present in the g1 IVC (as indicated by the presence of ions such as SiIV, CIII and CIV), because O is so strongly coupled to H through charge exchange interactions, the ionization corrections relating N(OI)/N(HI) to the metallicity [O/H] are small for values of log N(HI) > 19.5 (Viegas 1995), which applies to the M 15 sight-lines. Thus, the value of [OI/HI] approximates to that of [O/H]. We define the metallicity of [O/H] = (log [N(OI)/N(HI)] +12) – O$_\odot$, in which O$_\odot$ is the solar abundance of O given by Asplund et al. (2009), and derive a mean value of [O/H] = −1.22 ± 0.44 for the IVC gas using the values of column density listed in Table 3. This would suggest that the (neutral) IVC gas has a low value of metallicity (i.e. ∼6% of solar). To check on this result we repeat the same calculation for NI, which is also a good tracer of neutral gas for which we

Table 4. Predicted and observed high ion column density ratios for different ionization models.

Ionization method	Ion ratio	Predicted ratio	g1 cloud	M5-HVC[1]	Complex M-HVC[2]
Radiative cooling[a].....	N(CIV)/N(SiIV)	8.7–33.0	3.9 ± 1.5	4.2 ± 0.7	<1.0
	N(CIV)/N(NV)	0.9–2.7	>10.5	>3.3	<1.05
	N(CIV)/N(OVI)	0–0.2	0.83 ± 0.37	>2.1	<0.35
Conductive interface[b].....	N(CIV/N(SiIV)	5.5–30.9	3.9 ± 1.5	4.2 ± 0.7	<1.0
	N(CIV)/N(NV)	0.8–2.6	>10.5	>3.3	<1.05
	N(CIV)/N(OVI)	0.1–0.9	0.83 ± 0.37	>2.1	<0.35
Turbulent mixing layers[c].....	N(CIV/N(SiIV)	0.9–28.8	3.9 ± 1.5	4.2 ± 0.7	<1.0
(non-equilibrium ionization)	N(CIV)/N(NV)	7.4–29.5	>10.5	>3.3	<1.05
	N(CIV)/N(OVI)	1.1–7.4	0.83 ± 0.37	>2.1	<0.35
Shock ionization[d].....	N(CIV/N(SiIV)	1.3–33.0	3.9 ± 1.5	4.2 ± 0.7	<1.0
	N(CIV)/N(NV)	0.7–38.6	>10.5	>3.3	1.0
	N(CIV)/N(OVI)	0–1.1	0.83 ± 0.37	>2.1	<0.35
Halo SNR[e].....	N(CIV/N(SiIV)	–	3.9 ± 1.5	4.2 ± 0.7	<1.0
	N(CIV)/N(NV)	1.8–9.0	>10.5	>3.3	1.0
	N(CIV)/N(OVI)	0.1–3.0	0.83 ± 0.37	>2.1	<0.35

Notes. 1 = –142 km s^{-1} HVC towards M5 (Zech et al. 2008), 2 = –131 km s^{-1} Complex M HVC towards Mrk 421 (Yao et al. 2011). [a] = Edgar and Chevalier (1986), [b] = Borkowski et al. (1990), [c] = Slavin et al. (1993), [d] = Dopita and Sutherland (1996), [e] = Shelton (1998).

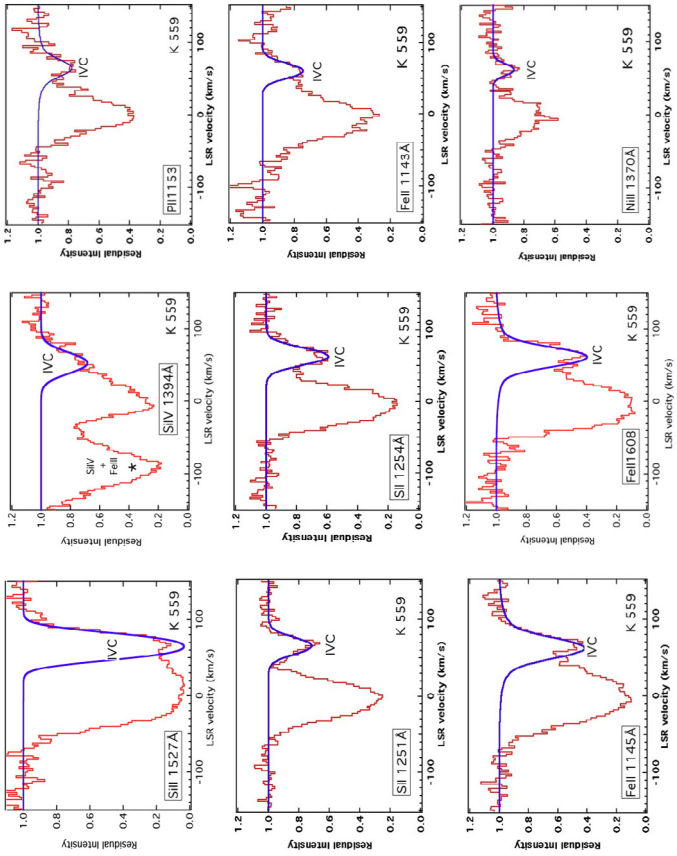

Fig. 4. Normalized UV absorption line profiles of the SiII, SiIV, PII, SII, FeII and NiII ions exhibiting IVC absorption towards the star K 559 at a velocity of $V_{\rm lsr}$ ∼ +61.5 km s^{-1}. See Fig. 1 for further details.

can assume N(NI)/N(HI) ∼ [N/H]. We find a value of [N/H] = −1.21 ± 0.38, which is almost identical to the metallicity value found for O in the neutral gas. We note however that N(NII) > N(I) in this sight-line, thus indicating that substantial amounts of N are also present in the ionized HII gas in this sight-line, and thus our presently derived metallicity value for N is only applicable in the neutral (HI) gas regions. More importantly, these derived metallicity values are both very low when compared to those derived for other IVCs such as the Upper & Lower IV Arch and the Pegasus-Pisces Arch (Wakker 2001; Richter 2006). This may be an indicator of the origin of the g1 cloud, which will be discussed at the end of this section.

Ions of the other elements observed towards the g1 IVC may be formed in both neutral and more ionized regions, such that an ionization correction for the ion fraction that resides within the ionized gas component is required in order to estimate the *absolute* metallicity value of each element with respect to the *total* column density of both neutral and ionized hydrogen [i.e. N(HI) + N(HII)]. Although ionization corrections for the observed ion column densities can be estimated on theoretical grounds using photoionization models such as CLOUDY (Ferland et al. 1998; Collins et al. 2003), such calculations require many assumptions about the nature of the cloud environment and cloud size. These assumptions may include the nature of the ionizing radiation field, the local gas density, the fractional depletion onto dust grains, whether photoionization itself, as opposed to shock or collisional ionization, is the dominant ionizing mechanism and whether all ionization stages of the various ions have been accounted for in the UV observations. Given this list of (perhaps substantial) uncertainties, we choose instead to investigate the gas metallicity by deriving *relative* values of abundance for the various ions and then comparing these ratios to their corresponding solar abundance ratios as listed by Asplund et al. (2009). Since we are dealing with relative rather than absolute abundances, this analysis method has the advantage of eliminating the problem of the usual mis-match between UV and radio beam sizes. This type of relative abundance analysis has been successfully carried out for the HVC gas seen towards M 13 (Welsh et al. 2011), Complex C (Tripp et al. 2003; Collins et al. 2007) and towards HVC 291.2-41.2 by Lehner et al. (2001).

We start with the assumption that the column density values for the IV components listed in Table 3 for the various transitions of C, Si, S, Al, P, Fe and Ni represent their dominant ion stages in this interstellar sight-line. We note that this is probably not the case for Al and Fe, which may be present in the unobserved line of Al III or, depleted onto dust grains. Similarly

this is also the case for O, for which (due to the presence of highly ionized gas in this IVC) appreciable amounts of (unobserved) OII and OIII may be present. Alternately, for C, N and Si we are confident that we have observed all of the respective ions present in the g1 cloud. Thus, for element C we assume that N(C) = N(CI) + N(CII) + N(CIII) + N(CIV), for element N we assume $N(N)$ = N(I) + N(II) and for Si that N(Si) = N(SiII) + N(SiIII) + N(SiIV). We then compare the column density ratio values of N(C)/N(N), N(Si)/N(N) and N(C)/N(Si) with their corresponding solar abundance ratios given by Asplund et al. (2009). We find observed relative abundance ratios of C to N (here defined as $[C/N]_{rel}$) = −0.45 ± 0.19, that of Si to N (i.e. $[Si/N]_{rel}$) = −0.33 ± 0.21 and C to Si (i.e. $[C/Si]_{rel}$) = −0.12 ± 0.22. These three measurements of relative abundance ratios are all consistent with sub-solar values, as was indicated previously from the observed [O/H] and [N/H] column density ratios. Similarly we find low relative abundance ratio values for $[Al/N]_{rel}$ = −0.24 ± 0.13, $[Ni/N]_{rel}$ = −0.39 ± 0.12 and $[Fe/N]_{rel}$ = −0.45 ± 0.11, whereas we find higher ratio values for $[S/N]_{rel}$ = +0.33 ± 0.10 and $[P/N]_{rel}$ = +0.55 ± 0.20. In order for sulfur and potassium to to match the low relative abundance ratio values measured for the other elements with respect to N, it would require an appreciable column density from the saturated and heavily blended NIII λ989 Å absorption line. Thus taken as a whole, our data are consistent with the majority of the IVC gas possessing less than solar relative abundances with respect to N, which itself is of a low ([N/H]) metallicity value.

We note two important aspects of the present case of the g1 cloud IVC gas. Firstly, both the low and high ionization gas is moving *away* from the galactic disk, and secondly the IVC gas appears to have less than solar metallicity as measured from the [OI/HI] and [NI/HI] column density ratios. A widely accepted explanation for low abundances in IVCs and HVCs is that the gas is of an extragalactic origin that is perhaps halo gas falling onto the Galactic plane (Collins et al 2003; Shull et al. 2009). Based on the positive velocity of the g1 cloud, it may be that this low metallicity cloud has already been accreted towards our galaxy and has passed through the disk such that it is now moving away from the plane. A similar scenario has been forwarded by Lockman et al. (2008) to explain the observed motion of the Smith Cloud, which is an HVC moving with a velocity of +100 km s^{-1}.

4. Conclusion

We have presented medium resolution UV absorption observations of the 10.4 kpc sight-line to two stars in the M 15 globular cluster. We have detected absorption components at V_{lsr} ∼ +61.5 km s^{-1} in the profiles of the CI, CII, CII*, CIV, NI, NII, OI, OVI, AlII, SiII, SiIII, SiIV, PII, SII, FeII, FeIII and NiII ions whose origin is thought to arise in the g1 Intermediate Velocity Cloud of distance 1.8 to 3.8 kpc. We have fit these IV components with best-fit absorption models to derive column density values for each ion measured towards both stars. We have derived near identical ion column density values along *both* sight-lines, such that our UV data does not reveal the significant small-scale structure that was reported previously for the g1 cloud using NaI absorption measurements by Meyer & Lauroesch (1999) and by HI emission measurements by Smoker et al. (2002b). The difference between the findings derived from the NaI/HI, radio and the present UV data could be due to the UV lines sampling a far wider range of temperature, ionization and velocity than that encompassed by the NaI and HI observations.

We have compared the measured high ion column density ratios of N(CIV)/N(SiIV) = 3.9 ± 1.5, N(CIV)/N(OVI) = 0.83 ± 0.37 and N(CIV)/N(NV) > 10.5 to the ratios predicted by several possible ionization mechanisms. These three ratio values are consistent with what may be expected from turbulent mixing layers, shock ionization or from a halo SNR origin. If the highly ionized boundary to the g1 cloud is due to its interaction with passage through the surrounding halo gas, then we would expect that some form of collisional ionization model (such as turbulent mixing layers of shock ionization) might be appropriate to explain our data. We note that our observed value of N(CIV)/N(OVI) = 0.83 ± 0.37 is consistent with recent hydrodynamic simulations of HVCs traveling through a hot tenuous medium in the galactic halo (Kwak et al. 2011).

The neutral IVC gas has absolute metallicity values of [O/H] = −1.22 ± 0.44 and [N/H] = −1.21 ± 0.38. These near identical values suggest that the neutral IVC gas has a low metallicity value of ∼6% solar. We find that the column density ratio values of N(C)/N(N), N(Si)/N(N) and N(C)/N(Si) possess lower than solar relative abundances, as do the ratio values for N(Al)/N(N), N(Ni)/N(N) and N(Fe)/N(N), but not the ratios of N(S)/N(N) and N(P)/N(N). Taken as a whole, our data are consistent with the majority of the IVC gas possessing less than solar relative abundances with respect to N, which itself is of a low ([N/H]) metallicity value.

Finally, we note that the g1 cloud is moving *away* from the galactic plane and that its constituent gas has a low value of metallicity. These two points may be explained if the cloud has already accreted towards our galaxy and has passed through the disk, such that it is currently moving away from the plane. A similar origin has recently been forwarded for the Smith HVC by Lockman et al. (2008).

Acknowledgements. We acknowledge all of the dedicated team of engineers, technicians, scientists and astronauts who contributed to the success of the the STS-125 servicing mission to the *Hubble* Space Telescope. We thank Dr. Robin Shelton for useful discussions concerning hydrodynamic simulations of high ion production in HVCs. We also thank the HST-COS science team for their advice and financial support through NASA GSFC grant 005118.

References

Asplund, M., Grevesse, N., Sauval, A., & Scott, P. 2009, ARA&A, 47, 481
Bianchi, L., Bohlin, R., Catanzaro, G., et al. 2001, AJ, 122, 1538
Borkowski, K., Balbus, S., & Fristrom, C. 1990, ApJ, 355, 501
Bregman, J. 1980, ApJ, 236, 577
Collins, J., Shull, J. M., & Girouz, M. 2003, ApJ, 585, 336
Collins, J., Shull, J. M., & Giroux, M. 2004, ApJ, 605, 216
Collins, J., Shull, J. M., & Giroux, M. 2007, ApJ, 657, 271
Danly, L., Lockman, F., Meade, M., & Savage, B. 1992, ApJS, 81, 125
Dixon, W. V. D., Chayer, P., Welsh, B. Y., & Green, J. 2011, BAAS, 338, 15
Dopita, M., & Sutherland, R. 1996, ApJS, 102, 161
Drukier, G., Slavin, S., Cohen, H., et al. 1998, AJ, 115, 708
Durrel, P., & Harris, W. 1993, AJ, 105, 4
Edgar, R., & Chevalier, R. 1986, ApJ, 310, L27
Ferland, G., Korista, K., Verner, D., et al. 1998, PASP, 110, 761
Fox, A., Wakker, B., Savage, B., et al. 2005, ApJ, 630, 332
Flynn, C., & Morello, O. 1997, MNRAS, 286, 617
Gibson, B., Giroux, M., Penton, S., et al. 2001, AJ, 122, 3280
Gnat. O., Sternberg, A., & McKee, C. 2010, ApJ, 718, 1315
Howk, J. C., Sembach, K., & Savage, B. 2003, ApJ, 586, 249
Indebetouw, R., & Shull, J. M. 2004, ApJ, 605, 205
Kennedy, D., Bates, B., Keenan, F., et al. 1998, MNRAS, 297, 849
Kerr, F., & Knapp, G. 1972, AJ, 77, 5
Kwak, K., & Shelton, R. 2010, ApJ, 719, 523
Kwak, K., Henley, D., & Shelton, R. 2011, ApJ, 739, 30
Lehner, N., & Howk, J. C. 2010, ApJ, 709, L138
Lehner, N., Rolleston, W., Ryans, R., et al. 1999, A&AS, 134, 257
Lehner, N., Keenan, F., & Sembach, K. 2001, MNRAS, 323, 904

Little, J., Dufton, P., Keenan, F., & Conlon, E. 1994, ApJ, 427, 267
Lockman, F. J., Benjamin, R., Heroux, A., & Langston, G. 2008, ApJ, 679, L21
Lodders, K. 2003, ApJ, 591, 1220
Lyons, M., Bates, B., & Kemp, S. 1994, A&A, 286, 535
Meyer, D., & Lauroesch, J. 1999, ApJ, 520, L103
Mooney, C., Rolleston, W., Keenan, F., et al. 2004, A&A, 419, 1123
Osterman, S., Green, J., Froning, C., et al. 2011, Ap&SS, in press [arXiv:1012.5827]
Richter, P. 2006, Rev. Mod. Astron., 19, 31
Richter, P., Savage, B., Wakker, B., Sembach, K., & Kalberla, P. 2001a, ApJ, 549, 281
Richter, P., Sembach, K., Wakker, B., et al. 2001b, ApJ, 559, 318
Savage, B., & Wakker, B. 2009, ApJ, 702, 1472
Savage, B., Sembach, K., Wakker, B., et al. 2003, ApJS, 146, 125
Sembach, K., Savage, B., Lu, L., & Murphy, E. 1999, ApJ, 515, 108
Sembach, K., Gibson, B., Fenner, Y., & Putman, M. 2002, ApJ, 572, 178
Sembach, K., Wakker, B., Savage, B., et al. 2003, ApJS, 146, 165
Shapiro, P., & Field, G., 1976, ApJ, 205, 762
Shelton, R. 1998, ApJ, 504, 785
Shull, J. M., Jones, J., Danforth, C., & Collins, J. 2009, ApJ, 699, 754
Shull, M. J., Stevans, M., Danforth, C., et al. 2011, ApJ, 739, 105
Slavin, J., Shull, J. M., & Begelmen, M. 1993, ApJ, 407, 83
Smoker, J., Keenan, F., Lehner, N., & Trundle, C. 2002a, A&A, 387, 1057
Smoker, J., Haffner, L., Keenan, F., et al. 2002b, MNRAS, 337, 385
Spitoni, E., Recchi, S., & Matteucci, F. 2008, A&A, 484, 743
Tripp, T., & Song, L. 2011, ApJ, in press [arXiv:1101.1107]
Tripp, T., Wakker, B., Jenkins, E., et al. 2003, AJ, 125, 3122
Vallerga, J. V., Vedder, P., Craig, N., & Welsh, B. Y. 1993, ApJ, 411, 729
Viegas, S. M. 1995, MNRAS, 276, 268
Wakker, B. 1991, A&A, 250, 499
Wakker, B. 2001, ApJS, 136, 537
Wakker, B., York, D., Wilhelm, R., et al. 2008, ApJ, 672, 298
Welsh, B. Y., & Lallement, R. 2005, A&A, 436, 615
Welsh, B. Y., Wheatley, J., & Lallement, R. 2009, PASP, 121, 606
Welsh, B. Y., Wheately, J., & Lallement, R. 2011, PASP, 123, 914
Yao, Y., Shull, J. M., & Danforth, C. 2011, ApJ, 728, L16
Zech, W., Lehner, N., Howk, J., et al. 2008, ApJ, 679, 460